

Encounter of the Ulysses Spacecraft with the Ion Tail of Comet McNaught

M. Neugebauer¹, G. Gloeckler², J. T. Gosling³, A. Rees⁴, R. Skoug⁵,
B. E. Goldstein⁶, T. P. Armstrong⁷, M. R. Combi⁸, T. Mäkinen⁹, D. J. McComas¹⁰,
R. von Steiger¹¹, T. H. Zurbuchen¹², E. J. Smith¹³, J. Geiss¹⁴, and L. J. Lanzerotti¹⁵

ABSTRACT

Comet McNaught was the brightest comet observed from Earth in the last 40 years. For a period of five days in early February 2007, four instruments on the Ulysses spacecraft directly measured cometary ions and key properties of the interaction of the comet's ion tail with the high-speed solar wind from the polar regions of the Sun. Because of the record-breaking duration of the encounter, the data are unusually comprehensive. O^{3+} ions were detected for the first time at a comet, coexisting with singly charged molecular ions with mass in the range 28-35 amu. The presence of magnetic turbulence and of ions with energies up to ~ 200 keV indicate that at a distance of ~ 1.6 AU from the comet nucleus, the ion tail of comet McNaught had not yet reached equilibrium with the surrounding solar wind.

Subject headings: comet tails, solar wind, plasma, abundances

1. Introduction

In early February 2007, comet C/2006 P1 McNaught had passed through perihelion and was on its way back to the outer solar system, while the Ulysses spacecraft was on its inbound passage of the southern solar polar region. On February 3 and 4, the comet and the spacecraft were nearly radially aligned with respect to the Sun, with a Ulysses-Sun-comet angle $< 1^\circ$. At the time, the comet was 0.7 AU from the Sun, while Ulysses was at 2.4 AU.

The immersion of Ulysses in cometary material is demonstrated in Fig. 1. The top panel displays energy/charge spectra in units of keV/charge measured by the SWOOPS experiment (Bame et al. 1992). For over a year before the comet encounter, Ulysses had been in the high-speed ($> 700 \text{ km s}^{-1}$) solar wind typical of the solar polar regions at solar activity minimum (Geiss et al. 1995; McComas et al. 2000). At the beginning and end of the spectrogram in the top of Fig. 1, the red contours show solar wind protons (H^+) with a speed of $\sim 780 \text{ km s}^{-1}$. The yellow contours at a factor ~ 2 higher energy/charge are alpha particles (He^{++}), with a slightly higher speed than the protons. Beginning on February 5, the solar wind speed and proton density declined, eventually reaching minima of

¹Lunar and Planetary Laboratory, University of Arizona, Tucson, AZ 85721; mneugeb@lpl.arizona.edu

²University of Michigan, 2455 Hayward St., Ann Arbor, MI 48109, and University of Maryland, College Park, MD 2074

³LASP, University of Colorado, Boulder, CO 80303

⁴Imperial College, London, UK

⁵Los Alamos National Laboratory, Los Alamos, NM 87545

⁶Jet Propulsion Laboratory, California Institute of Technology, Pasadena, CA 91109

⁷Fundamental Technologies, LLC, 2411 Ponderosa Dr., Suite A, Lawrence, KS 66046

⁸University of Michigan, 2455 Hayward St., Ann Arbor, MI 48109

⁹Finnish Meteorological Institute, P.O. Box 503, FIN-00101, Finland

¹⁰Southwest Research Institute, P.O. Drawer 28510, San Antonio, TX 78228

¹¹International Space Science Institute, Hallerstrasse 6, CH-3012, Bern, Switzerland

¹²University of Michigan, 2455 Hayward St., Ann Arbor, MI 48109

¹³Jet Propulsion Laboratory, California Institute of Technology, Pasadena, CA 91109

¹⁴International Space Science Institute, Hallerstrasse 6, CH-3012, Bern, Switzerland, and University of Bern, CH-3012, Bern, Switzerland

¹⁵Dept. Physics, New Jersey Institute of Technology, Newark, NJ 07102

$\sim 360 \text{ km s}^{-1}$ and 0.0018 cm^{-3} on February 7. At the same time, both the proton and alpha particle temperatures rose. Traces of picked-up cometary ions with greater energy/charge were observed on February 7. The possibility that the disturbance was caused by solar activity is ruled out because the temperature signature was opposite to what would have been observed as a result of a typical coronal mass ejection (Gosling, Pizzo, & Bame 1973) and because there was no unusual solar activity at high southern latitudes during this period.

The detection of cometary ions by the SWICS instrument (Gloeckler et al. 1992) is shown in the middle panel of Fig. 1 where mass/charge (m/q) is plotted versus time. At the beginning and end of the interval, almost all ions had $m/q \leq 4$, corresponding to highly charged heavy ions in the solar wind. At higher m/q , there was the normal presence of singly charged pickup ions created inside the orbit of Ulysses from interstellar and ‘inner source’ neutral atoms (Gloeckler et al. 2000a; Gloeckler & Geiss 1998). Near the beginning of February 5, many ions of cometary origin appeared. The red contour at $m/q = 16$ is O^+ .

The bottom panel in Fig. 1 shows the fluxes of energetic ions in the three lowest-energy channels of the HISCALE instrument (Lanzerotti et al. 1992). Signals above background were detected at the start and end of the event, but not in the middle.

Fig. 2 shows the gas production rate (Q) of comet McNaught versus radial distance (R in AU) as determined from nine images of the H Lyman-alpha coma taken with the SOHO SWAN instrument (Bertaux et al. 1999; Combi et al. 2005; Mäkinen & Combi 2005) between January 30 and February 11. A least squares fit of the gas production rate to a power law in solar distance yields $Q = 9.2 \times 10^{29} R^{-1.73} \text{ (s}^{-1}\text{)}$. Deviations from this fit ranged from -11% to $+7.5\%$.

In the remainder of this report we examine several aspects of the physics of the interaction between the comet and the solar wind and compare the measurements at comet McNaught with those at two of the three previous encounters of spacecraft with comet tails.

2. Detailed Observations

Fig. 3 presents plasma parameters calculated from the SWOOPS and magnetometer (Balogh et al. 1992) data. From top to bottom are plotted (a) proton speed, (b) proton density, (c) proton kinetic temperature, (d) the magnitude of the magnetic field, (e, f, g) the components of the magnetic field in the RTN (Radial, Tangential or longitudinal, Normal or latitudinal) coordinate system, and (h) the angle between the magnetic field and the solar radial direction. Before ~ 0600 on February 4 and after 1200 on February 9, the parameters were all typical of the high-speed polar solar wind. The relative steadiness of the field

magnitude together with the large variations in the components of the field are signatures of transverse Alfvén waves. From panel (h) note that during these periods the field, on average, pointed outward from the Sun, as expected for the southern hemisphere for the current phase of the solar magnetic cycle. Several times a day the transverse fluctuations in the field were sufficient for the angle briefly to exceed 90° , i.e., for the field to point inward toward the Sun.

The first detection of the comet is the slight decline in speed and the small increases in density, temperature, and field magnitude on February 4. Some compressional waves can also be seen in the variability of the field magnitude. Those signatures, although weak, are all consistent with the start of mass loading of the wind by the ionization and pickup of cometary material. As ionized cometary material was added to the solar wind, conservation of momentum and energy required the plasma to be slowed, compressed, and heated. The unstable velocity distributions of the picked-up ions in turn generated a variety of wave modes, including ion-cyclotron waves, which caused variations in field magnitude.

The situation changed significantly on February 5. The deceleration of the wind increased and the proton density started a steep decline. Even though the protons continued to be compressed as the wind slowed, they were rapidly removed from the flow by charge-exchange collisions with cometary molecules and atoms. Beginning early on February 5, the field departed from its generally outward orientation to point nearly radially inward, indicating that Ulysses had passed into the region where the field was draped around the cometary obstacle, as first proposed by Alfvén (Alfvén 1957). No shock wave was detected there, or anywhere else during the encounter.

The field remained mostly in the draped configuration until ~ 0900 on February 9. There is no indication that Ulysses passed through the center of the ion tail to emerge on the other side with the draped field having an opposite orientation. There were, however, many short reversals of the field from nearly radially inward to nearly radially outward, and then back again. A possible cause of this filamentary structure is the incorporation in the draping process of the occasional excursions of the interplanetary field to inward directions caused by upstream Alfvénic fluctuations. Also, when the reversed (i.e., outward) field coincided with local flow-speed minima, such as in the middle of February 7, the reversal could have arisen from the distortion of the field by the motion of slow plasma relative to the adjacent faster plasma if the field lines threaded both plasmas.

The profiles of the plasma parameters were not monotonic on either ingress or egress. In particular, note the temporal increases in speed and density centered on 1400 on February 5 and 0800 on February 8 and the decrease around 1300 on February 8. The variations were probably associated with changes of the gas production rate of the comet as indicated in

Fig. 2.

After the speed minimum, the recovery of the plasma parameters was not a mirror image of the drop to minimum speed. The time from first detection of the comet interaction to the speed minimum was > 2.5 days, while the recovery required < 2 days. This difference is significantly greater than can be explained by the 10% decrease of the comet-spacecraft separation between the start and the end of the event. For a given speed, the density and temperature were higher on the way out of than on the way into the tail. Although the magnetic field retained its draped configuration on the way out, the wave activity, both compressional and transverse, were significantly increased. The energetic particle flux was also greater on egress than on ingress. Although those differences could have resulted from variations in the activity of the comet, they are all consistent with compression of the exit side of the tail. The transverse motion of the comet around the Sun is in the correct direction to provide such compression, but whether or not the $\sim 25 \text{ km s}^{-1}$ transverse speed is sufficiently large requires further study and modeling.

The data presented in Fig. 4 clearly show the relation between the slowdown of the solar wind speed and the accumulation of pickup ions. The top panel shows the speed of solar wind He^{++} ions as measured by SWICS. The middle panel shows the time profile of O^+ detected by SWICS. The amount of O^+ began to rise above its background solar-wind level during February 4, and closely complemented the speed profile in the top panel; the speed was lowest when the density of O^+ was greatest. The bottom panel of Fig. 4 shows the phase space density of H^+ ions with speeds between 1.55 and 2.00 times the speed of the solar wind. Almost all the ions in that speed range would have been created in the solar wind and then accelerated as they were picked up by and spiraled around the interplanetary magnetic field. Some of the pickup protons probably originated in hydrogen-bearing cometary molecules such as water, while the rest were of interstellar origin (Gloeckler et al. 1993).

Fig. 5 shows mass spectra detected by SWICS summed over the period February 6 through 9. These spectra show an unusual mixture of cometary molecular ions in the m/q range 28-35 amu/e together with singly, doubly, and even triply charged atomic ions. Further study is required to determine whether the O^{3+} ions came from the ionization of O^{2+} or from the multi-stage neutralization of the O^{7+} and O^{6+} ions in the solar wind (Cravens 1997).

3. Comparison to Other Comet Tail Encounters

There have been three other encounters of spacecraft with the tails of identified comets: the ICE spacecraft with comet Giacobini-Zinner (GZ) (Bame et al. 1986; Hynds et al. 1986;

Ipavich et al. 1986; Ogilvie et al. 1986; Smith et al. 1986; von Roseninge, Brandt, & Farquhar 1986) and Ulysses with comets Hyakutake (Gloeckler et al. 2000b; Jones, Balogh, & Horbury 2000; Riley et al. 1998) and McNaught-Hartley (Gloeckler et al. 2004). Table 1 summarizes some of the properties of two of those encounters and compares them to the Ulysses encounter with comet McNaught. Comparison to the McNaught-Hartley encounter is not included because that comet’s tail was strongly distorted by a coronal mass ejection.

The parameters of the GZ encounter were quite different from those of McNaught and Hyakutake. GZ was much less active than the other two comets. The encounter with Hyakutake occurred at a much greater down-tail distance than the encounter with McNaught, and both were at orders of magnitude greater distances than the GZ encounter.

In Table 1 the widths of the disturbances were calculated from the time elapsed between the start and the end of the disturbances multiplied by the relative transverse speeds of the comets and the spacecraft. It might be expected that the tail diameter would increase with the R^{-2} expansion of the solar wind. That effect, together with the difference in comet gas production rates, readily explains why the GZ tail was much narrower than the other two. Comparison of the tail widths of McNaught and Hyakutake do not fit that picture, however. The difference might lie in that McNaught was about twice as far from the Sun when the tail material left the comet than was Hyakutake, corresponding to a factor of four difference in the density and the momentum flux of the solar wind. Thus Hyakutake’s tail may have been narrower due to confinement of the plasma by a denser wind which increased the charge exchange rate close to the comet. Note, however, that for both encounters Ulysses cut through a chord of the tail without passing through its center, but the abundance of cometary ions and the large depletion of solar-wind protons suggest that both spacecraft did penetrate fairly deeply into the tails.

The minimum velocity in the tail depended strongly on the distance of the spacecraft from the nucleus, indicating continued acceleration of the plasma down the tail. At Hyakutake, the velocity shear between the flow in the tail and that in the surrounding solar wind had nearly disappeared.

During the brief encounter with GZ, water group ions (O^+ through H_3O^+) and some heavier molecular ions could be discerned. The O^+ signal was weaker than that of H_2O^+ and H_3O^+ . The Ulysses mass spectra at McNaught and Hyakutake were qualitatively similar to each other over the range $m/q = 6$ to 22 amu/e. However, $m/q > 25$ amu/e ions were not detected at Hyakutake, nor were significant amounts of O^{3+} . The O^{++}/O^+ counts ratio was 25% greater, and the C^+/O^+ counts ratio was about three times higher at Hyakutake than at McNaught. Taken together, the relative paucity of O^+ at GZ, the increase of O^{++}/O^+ , and the decrease of ions with $m/q > 25$ amu/e between McNaught and Hyakutake reflect

the dependence of ionization and dissociation rates on distance from the Sun together with continuing ionization and dissociation with distance down the tail. The higher C^+/O^+ count ratio at Hyakutake is consistent with the fact that McNaught has been reported to be relatively CO poor (2-4%) (Dello Russo et al. 2007), whereas Hyakutake had an unusually high CO abundance (20%) (Biver et al. 1999; DiSanti et al. 2003; Mumma et al. 1996).

The ion pickup process results in ion energies ranging up to $2mv^2$, where m is the ion mass and v is the speed of the fluid flow. Ions with energies above that maximum were observed throughout the GZ encounter (Hynds, et al. 1986; Ipavich, et al. 1986). Mechanisms proposed for the acceleration of pickup ions include acceleration at the upstream bow shock, compression of the plasma during mass loading, and second-order Fermi acceleration in the intense wave fields. At McNaught, the maximum energy for the dominant O^+ ion was below the threshold of the HISCALE detectors on February 5 and 6, and consequently no particles were recorded. When the velocity was higher, there were many more energetic particles on the exit side of the tail than on the entrance side. We interpret that asymmetry as acceleration of the pickup ions by the greater turbulence seen by the magnetometer on the exit side of the tail. At Hyakutake, where the acceleration of the tail plasma was nearly complete with little velocity shear between the tail and the surrounding solar wind, neither waves nor energetic particles were detected (Riley, et al. 1998). All told, the low minimum speed and the presence of waves and energetic particles show that at a distance of ~ 1.6 AU from the nucleus, the ion tail of comet McNaught had not yet come to equilibrium with the surrounding solar wind. This is in contrast to the tail of comet Hyakutake at a distance 3.4 AU where those features were not observed.

Work is ongoing to explain many of the detailed features in the data and to compare the observations at comet McNaught to models of the interaction of active comets with the solar wind.

We thank J. Harvey for information about solar activity and D. K. Yeomans for help with ephemerides. Ulysses and SOHO are cooperative missions between ESA and NASA. We gratefully acknowledge the personnel who have kept Ulysses, SOHO, and their instruments operating for over 16 and 10 years, respectively. The research reported here was supported by NASA and the Swiss National Science Foundation.

REFERENCES

- Alfvén, H. 1957, *Tellus*, 9, 92
Balogh, A., et al. 1992, *A&A Suppl.*, 92, 221

- Bame, S. J., et al. 1986, *Science*, 232, 356
- . 1992, *A&AS*, 92, 237
- Bertaux, J.-L., et al. 1999, *Space Sci. Rev.*, 87, 129
- Biver, N., et al. 1999, *AJ*, 118, 1850
- Combi, M. R., Mäkinen, J. T. T., Bertaux, J.-L., & Quermerais, E. 2005, *Icarus*, 177, 228
- Cravens, T. E. 1997, *Geophys. Res. Lett.*, 24, 105
- Dello Russo, N., Vervack Jr., R. J., Weaver, H. A., & Lisse, C. M. 2007, *IAU Circ.* 8816
- DiSanti, M. A., Mumma, M. J., Dello Russo, N., Magee-Sauer, K., & Griep, D. M. 2003, *J. Geophys. Res.*, 108, doi:10.129/2002JE001961
- Geiss, J., et al. 1995, *Science*, 268, 1033
- Gloeckler, G., et al. 2004, *ApJ*, 604, L121
- Gloeckler, G., et al. 2000a, *J. Geophys. Res.*, 105, 7459
- Gloeckler, G., & Geiss, J. 1998, *Space Sci. Rev.*, 86, 127
- Gloeckler, G., et al. 1992, *A&AS*, 92, 267
- 1993, *Science*, 261, 70
- . 2000b, *Nature*, 404, 576
- Gosling, J. T., Pizzo, V., & Bame, S. J. 1973, *J. Geophys. Res.*, 78, 2001
- Hynds, R. et al. 1986, *Science*, 232, 361
- Ipavich, F. M., et al. 1986, *Science*, 232, 366
- Jones, G. H., Balogh, A., & Horbury, T. S. 2000, *Nature*, 404, 574
- Lanzerotti, L. J., et al. 1992, *A&AS*, 92, 349
- Mäkinen, J. T. T., & Combi, M. R. 2005, *Icarus*, 177, 217
- McComas, D. J., et al. 2000, *J. Geophys. Res.*, 105, 10419
- Mumma, M. J., et al. 1996, *Science*, 272, 1310
- Ogilvie, K. W., Coplan, M. A., Bochsler, P., & Geiss, J. 1986, *Science*, 232, 374
- Riley, P., Gosling, J. T., McComas, D. J., & Forsyth, R. J. 1998, *J. Geophys. Res.*, 103, 1933
- Smith, E. J., et al. 1986, *Science*, 232, 382
- von Rosenvinge, T. T., Brandt, J. C., & Farquhar, R. W. 1986, *Science*, 232, 353

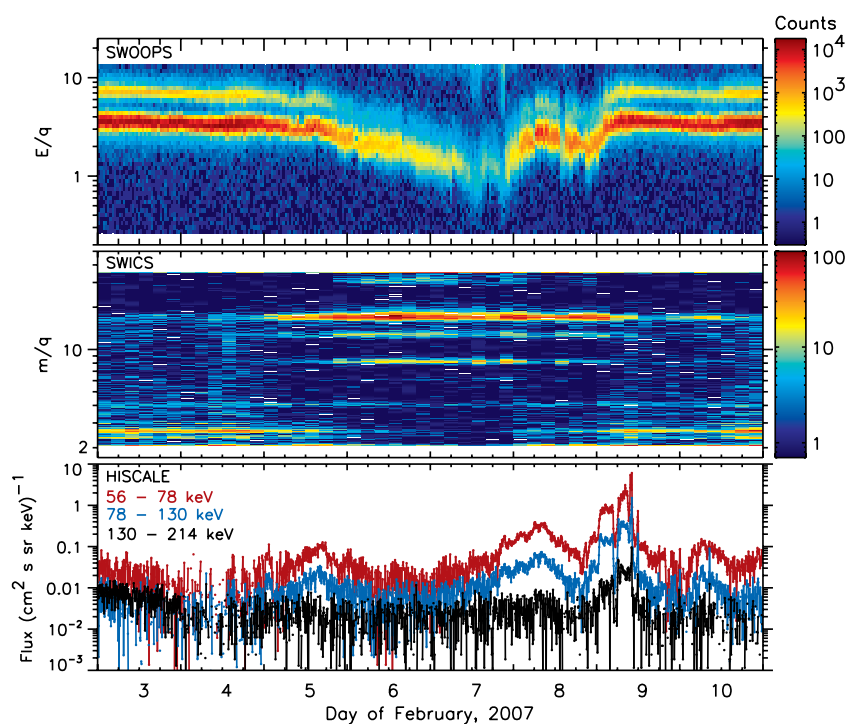


Fig. 1.— (Top) Energy/charge spectrogram of ions observed by SWOOPS. (Center) Mass/charge spectrogram of ions observed by SWICS. (Bottom) The fluxes of energetic particles in the three lowest-energy channels of the HISCALE instrument. The purpose of this display is to illustrate the correlations of the temporal variations detected by the three instruments. The parameters plotted in the two upper panels represent counting rates; for quantitative analyses, one should use the physical units presented in later figures.

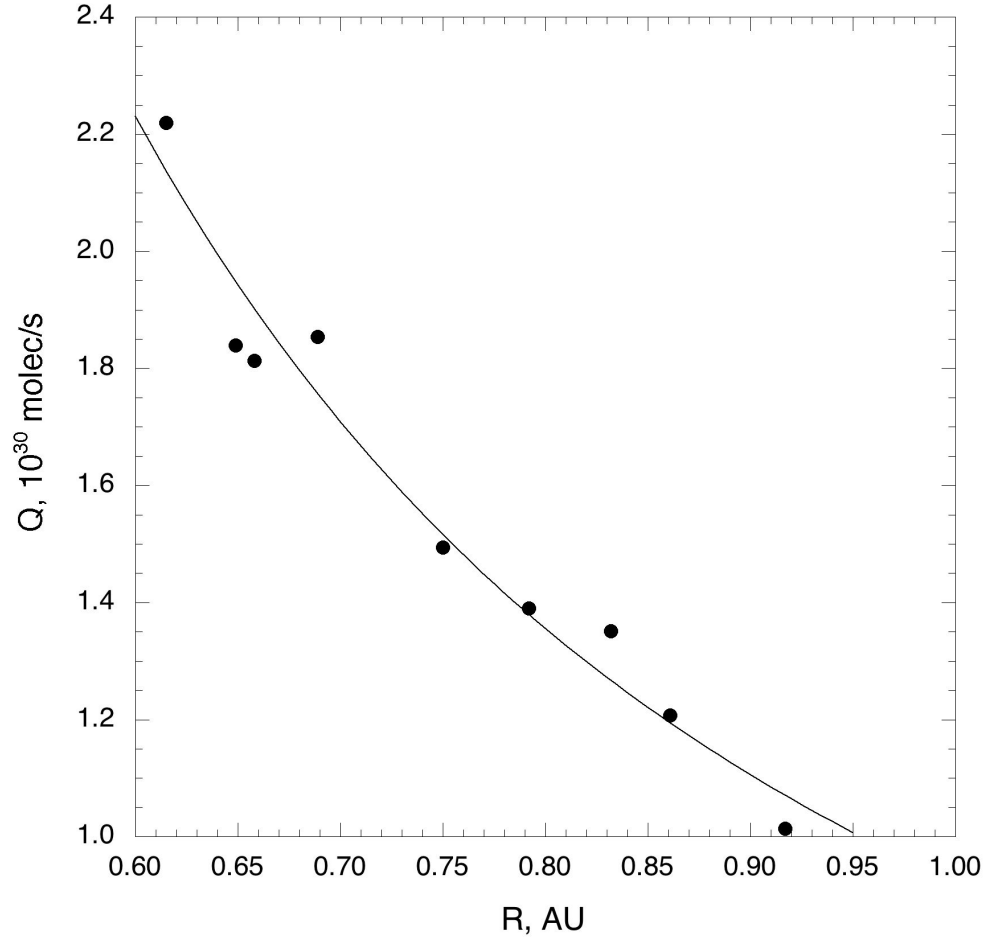


Fig. 2.— The water molecule production rate of comet McNaught (circles) as determined from H-Lyman-alpha images obtained by the SOHO SWAN experiment as a function of solar distance. The smooth curve shows a least-squares power-law fit to the data.

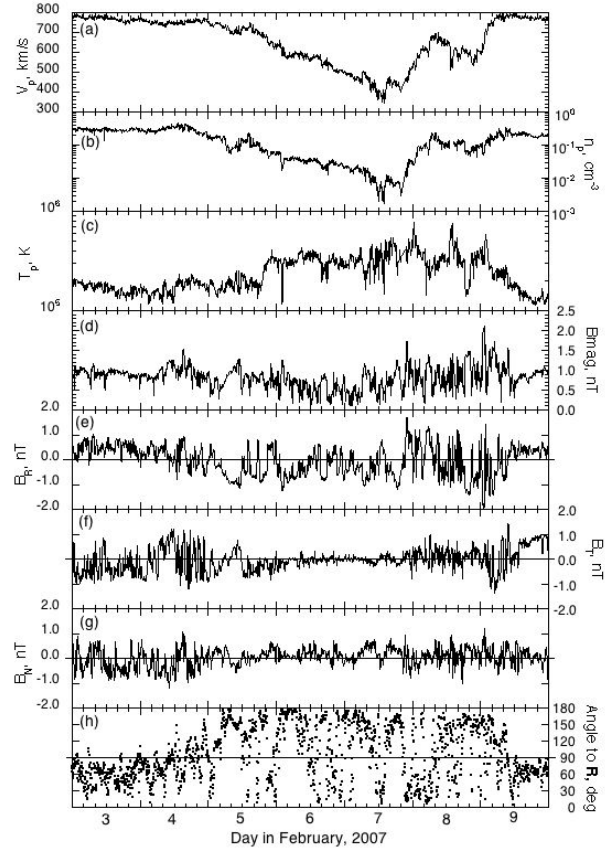


Fig. 3.— The three top panels show the speed, density, and kinetic temperature of protons detected by SWOOPS. The time resolution is 2 or 4 minutes, depending on the spacecraft data rate. Panel(d) shows the magnitude of the magnetic field, followed by the three components of the vector field, all at 5-minute resolution. The bottom panel displays the angle between the direction of the magnetic field and the outward radius vector from the Sun.

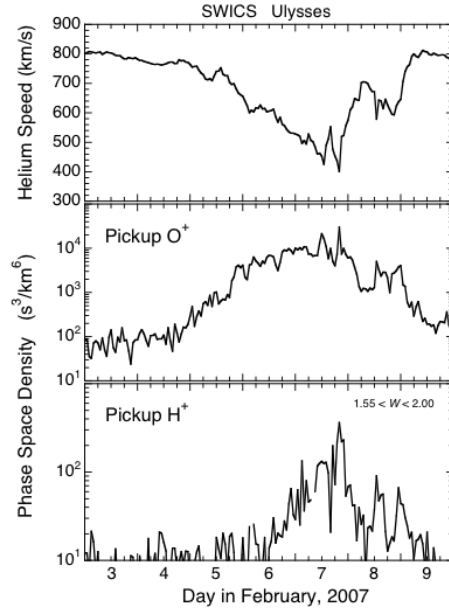


Fig. 4.— Ion parameters measured by SWICS. (Top) Speed of He^{++} ions. (Middle) Phase-space density of O^+ ions, summed over all speeds. (Bottom) Phase-space density of H^+ ions summed over the speed range 1.55 to 2.00 times the speeds of the He^{++} ions.

Table 1. Comparison of several properties of the ion tails of three comets

	Giacobini-Zinner	McNaught	Hyakutake
Year	1985	2007	1996
Solar distance of comet, AU	1.03	0.60 to 0.78	0.35
Nucleus-spacecraft distance	~ 8000 km	1.74 to 1.58 AU	3.4 AU
Gas production rate, s^{-1}	4×10^{28}	$1.4 \text{ to } \geq 2.2 \times 10^{30}$	$1 \text{ to } 2 \times 10^{30}$ (Refs 1, m2)
Disturbance width, km	3×10^5	1.2×10^7	6.3×10^6
Drop in proton density	No data	Factor ~ 100	Factor 8 (Ref 3)
Solar wind speed change, km s^{-1}	500 to ≤ 100 (Ref 4)	780 to 360	750 to 740 (Ref 3)
$m/q \geq 25$ amu/e?	Yes (Ref 5)	Yes	No
Waves and energetic particles?	Yes (Refs 6, 7)	Yes	No

References. — (1) Gloeckler et al. 2000b; (2) Jones et al 2000; (3) Riley et al. 1998; (4) Bame et al. 1986; (5) Ogilvie et al. 1986; (6) Hynds et al. 1986; (7) Ipavich et al. 1986

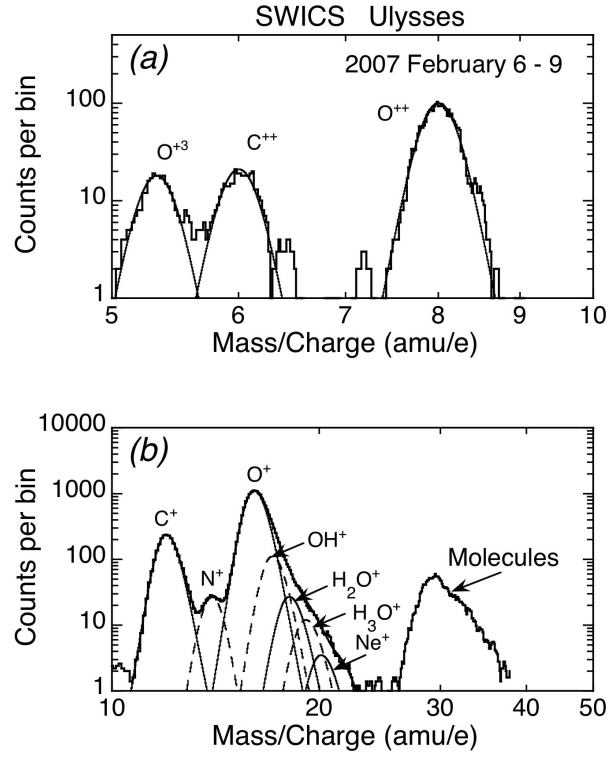


Fig. 5.— Mass/charge spectra measured by SWICS summed over the interval February 6 - 9.